

Quantum Adaptive Self-Attention for Financial Rebalancing: An Empirical Study on Automated Market Makers in Decentralized Finance

Chi-Sheng Chen

Omnis Labs

Cambridge, USA

m50816m50816@gmail.com

Aidan Hung-Wen Tsai

Omnis Labs

New York, USA

aidan@omnis.farm

Abstract—We formulate automated market maker (AMM) *rebalancing* as a binary detection problem and study a hybrid quantum–classical self-attention block, Quantum Adaptive Self-Attention (QASA). QASA constructs quantum queries/keys/values via variational quantum circuits (VQCs) and applies standard softmax attention over Pauli- Z expectation vectors, yielding a drop-in attention module for financial time-series decision making. Using daily data for BTCUSDC over Jan-2024–Jan-2025 with a 70/15/15 time-series split, we compare QASA against classical ensembles, a transformer, and pure quantum baselines under Return, Sharpe, and Max Drawdown. The QASA-Sequence variant attains the *best single-model risk-adjusted performance* (13.99% return; Sharpe 1.76), while hybrid models average 11.2% return (vs. 9.8% classical; 4.4% pure quantum), indicating a favorable performance–stability–cost trade-off.

Index Terms—Quantum machine learning, AMM, rebalancing, self-attention, hybrid quantum–classical models, DeFi backtesting.

I. INTRODUCTION

Decentralized finance (DeFi) has grown rapidly, with automated market makers (AMMs) becoming core primitives for on-chain liquidity provisioning [1]. AMMs implement constant-function designs (CFMMs) whose pricing and value properties have been formalized in recent theory, clarifying when pool prices are informative and how payoff replication arises [2], [3]. For liquidity providers (LPs), the practical challenge is *when and how to rebalance* under volatile, regime-switching markets. Empirical and theoretical studies further decompose LP P&L into market risk and *loss-versus-rebalancing (LVR)*, highlighting adverse selection and fee interplay [4], and show that concentrated-liquidity designs (e.g., Uniswap v3) require active management to maintain performance [5], [6].

Existing approaches to rebalancing span (i) transparent heuristics (fixed intervals, volatility triggers) and (ii) predictive machine learning. However, financial time series are noisy, non-stationary, and often governed by latent regimes [7], [8], making generalization fragile. While attention-based architectures such as Transformers [9] have delivered strong results in market microstructure and

forecasting—e.g., limit-order-book (LOB) prediction and multi-horizon forecasting [10]–[12]—their data hunger and overfitting risk can limit robustness in small-sample or rapidly shifting regimes typical for on-chain markets.

To address these challenges, we build on the *Quantum Adaptive Self-Attention (QASA)* block introduced in prior work [13] and tailor it to DeFi: compact descriptors (price changes, realized volatility, flow imbalance) are embedded into qubits and processed via VQCs; the measured expectations parameterize queries, keys, and values in a classical attention head [14]. From the feature-space viewpoint, quantum encodings act as (potentially) high-dimensional nonlinear maps [15]–[17], providing expressive interactions and inductive biases helpful for regime detection on noisy data, while remaining NISQ-friendly [18], [19]. Early quantum–attention explorations (e.g., quantum Transformers and quantum self-attention) suggest architectural viability across modalities [14]; in finance, quantum amplitude-estimation pipelines already deliver algorithmic speedups for option pricing [20].

a) Problem setup.: We cast rebalancing as a detection task. Labels are defined by thresholding deviations from a moving-average anchor:

$$y_t = \mathbb{I}\left(\frac{P_t}{\text{MA}_{20}(P_t)} - 1 > \tau_{\text{rebalance}}\right), \quad \tau_{\text{rebalance}} = 0.02, \quad (1)$$

where P_t is the spot price and MA_{20} a 20-period moving average. We evaluate strategies with standard trading metrics (Return, Sharpe, Max Drawdown) under identical fee and cooldown settings to ensure fair comparisons.

b) Contributions.: (i) We present, to the best of our knowledge, the *first application of prior QASA-style quantum self-attention* to DeFi/AMM rebalancing, adapting the block introduced in earlier work [13]—and related quantum self-attention designs [14]—to a detection-oriented rebalancing pipeline with DeFi-specific encodings (fees, ticks, cooldowns). (ii) We tailor QASA to AMM data via two practical instantiations: *QASA-Sequence* (short raw price windows) and *QASA-Hybrid* (raw windows plus engineered microstructure features), where Q/K/V are generated by variational quantum circuits and consumed

by a classical attention head. (iii) In a controlled 2024 backtest on three liquid crypto pairs with strict time-series splits and identical fee/cooldown settings, **QASA-Sequence** attains the best Sharpe (1.76) and return (13.99%), while hybrid variants outperform pure-quantum baselines on average.

II. RELATED WORK

a) *AMMs and concentrated liquidity.*: Automated market makers (AMMs) based on constant-function designs (CFMMs) have been analyzed from both protocol and economic perspectives. On the protocol side, Uniswap v2/v3 technical whitepapers specify the hardened oracle and concentrated-liquidity mechanisms that motivate rebalancing policy design under fees and tick ranges [1], [21]. Foundational analyses of CFMMs (e.g., price oracles, convexity, replication) formalize when on-chain prices are informative and how CFMM payoff surfaces relate to desired monotone payoffs [2], [3]. From the LP perspective, Milionis et al. decompose liquidity-provision P&L into market-risk and *loss-versus-rebalancing (LVR)* components, clarifying the role of volatility, depth and fees in profitability [4]. For Uniswap v3 specifically, strategic/tactical LP studies and empirical audits highlight the need for *active* management and regime awareness [5], [6].

b) *Learning for market regimes and volatility.*: Deep sequence models are widely used in financial time series. For high-frequency microstructure, CNN/LSTM hybrids (DeepLOB) established strong baselines on limit-order-book (LOB) data [22], and more recent Transformer-style architectures show further gains on LOB classification and forecasting [11]. For lower-frequency multi-horizon forecasting, the Temporal Fusion Transformer (TFT) offers competitive accuracy with interpretability and has been applied to realized-volatility prediction in turbulent markets [12], [23].

c) *Quantum ML and quantum attention.*: Quantum machine learning (QML) can be interpreted through feature-space/kernel lenses [16], [17], [24] and has been explored in finance via amplitude-estimation-based pricing/risk algorithms [20] and portfolio optimization. Closer to attention mechanisms, quantum Transformer variants and quantum self-attention modules have been proposed and evaluated on vision and NLP tasks [14], [25]. Departing from prior fully-quantum attention layers, our **QASA** combines compact feature encodings with variational quantum circuits (VQCs) to produce query/key/value statistics consumed by a *classical* attention head, aiming for NISQ-friendly training while preserving classical throughput [13].

III. METHODOLOGY

Task. Rebalancing as detection via the MA-anchored threshold in (1). We also consider alternative labels

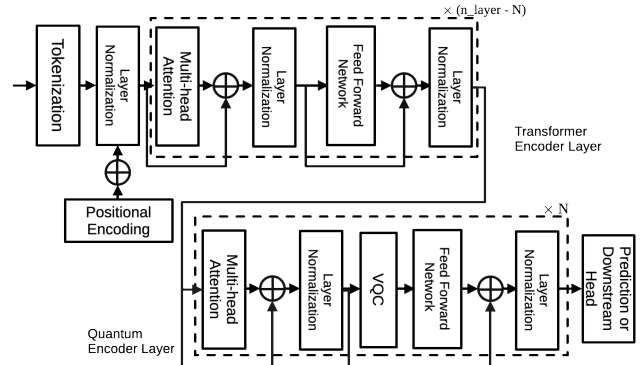


Fig. 1. QASA model.

(concentrated-liquidity band and price-change thresholds) in ablations.

Data. Daily candles for BTCUSDC from 2024-01-01 to 2025-01-01 (about 252 trading days); 70/15/15 time-series split (train/val/test). Five-run repeats quantify uncertainty.

a) *Features & quantum mapping.*: **Notation.** Let $t \in \mathbb{Z}$ index bars (e.g., 5-min). Denote mid/close price P_t , open O_t , high H_t , low L_t , close C_t , and volume V_t . Define log-returns $r_t := \log(P_t) - \log(P_{t-1})$ and the lag operator $\mathcal{L}^\ell x_t := x_{t-\ell}$.

Moving averages and volatility. For window $n \geq 1$,

$$\text{MA}_n(P_t) := \frac{1}{n} \sum_{j=0}^{n-1} P_{t-j}, \quad (2)$$

$$\text{EMA}_n(x_t) := \alpha_n x_t + (1 - \alpha_n) \text{EMA}_n(x_{t-1}), \quad \alpha_n = \frac{2}{n+1}, \quad (3)$$

$$\sigma_{n,t}^2 := \frac{1}{n-1} \sum_{j=1}^n (r_{t+1-j} - \bar{r}_{n,t})^2, \quad \bar{r}_{n,t} := \frac{1}{n} \sum_{j=1}^n r_{t+1-j}, \quad (4)$$

$$\hat{\sigma}_t^{\text{EWMA2}} := (1 - \lambda) r_t^2 + \lambda \hat{\sigma}_{t-1}^{\text{EWMA2}}, \quad \lambda \in (0, 1). \quad (5)$$

Price/MA ratios and momentum. For windows k, n ,

$$(\text{MA ratio}) \quad \rho_n(t) := \frac{P_t}{\text{MA}_n(P_t)} - 1, \quad (6)$$

$$(\text{k-step momentum}) \quad m_k(t) := \sum_{j=1}^k r_{t+1-j} = \log \frac{P_t}{P_{t-k}}. \quad (7)$$

Bollinger bands and ATR. For $(n_{\text{BB}}, k_{\text{BB}})$,

$$\mu_t := \text{MA}_{n_{\text{BB}}}(P_t), \quad s_t := \sqrt{\frac{1}{n_{\text{BB}}-1} \sum_{j=0}^{n_{\text{BB}}-1} (P_{t-j} - \mu_t)^2}, \quad (8)$$

$$U_t := \mu_t + k_{\text{BB}} s_t, \quad L_t := \mu_t - k_{\text{BB}} s_t, \quad (9)$$

$$\%b_t := \frac{P_t - L_t}{U_t - L_t} \in [0, 1], \quad z_t^{\text{BB}} := \frac{P_t - \mu_t}{k_{\text{BB}} s_t}. \quad (10)$$

True range and ATR over n_{ATR} :

$$\text{TR}_t := \max\{H_t - L_t, |H_t - C_{t-1}|, |L_t - C_{t-1}|\}, \quad (11)$$

$$\text{ATR}_t := \text{EMA}_{n_{\text{ATR}}}(\text{TR}_t), \quad a_t^{\text{rel}} := \frac{\text{ATR}_t}{P_t}. \quad (12)$$

Volume and microstructure proxies.

$$(\text{volume ratio}) \quad v_n(t) := \frac{V_t}{\text{MA}_n(V_t)} - 1, \quad (13)$$

$$(\text{signed volume}) \quad S_t := \text{sgn}(r_t) V_t, \quad (14)$$

$$\tilde{v}_n(t) := \frac{S_t}{\text{MA}_n(|S_t|) + \varepsilon}, \quad (15)$$

$$(\text{Amihud illiquidity}) \quad \mathcal{I}_n(t) := \frac{1}{n} \sum_{j=0}^{n-1} \frac{|r_{t-j}|}{V_{t-j} + \varepsilon}. \quad (16)$$

RSI, MACD, Lags and interactions. For a base feature set $\mathcal{F} = \{x_t^{(1)}, \dots, x_t^{(d)}\}$ and lag set $\mathcal{L} \subset \mathbb{N}$,

$$(\text{lag-augmented}) \quad \mathbf{x}_t := [x_t^{(1)}, \dots, x_t^{(d)}, \{\mathcal{L}^\ell x_t^{(j)}\}_{j, \ell \in \mathcal{F} \times \mathcal{L}}], \quad (17)$$

$$(\text{interactions}) \quad \mathcal{I}_{\text{pair}}(t) := \{x_t^{(i)} x_t^{(j)} : (i, j) \in \mathcal{S} \subset \{1, \dots, d\}^2\}. \quad (18)$$

From features to six scalars (for qubits). We aggregate engineered features into six continuous channels

$$\mathbf{s}_t = [s_t^{(1)}, \dots, s_t^{(6)}]$$

as

$$s_t^{(1)} := m_{k_m}(t) \quad (\text{momentum}), \quad (19)$$

$$s_t^{(2)} := \rho_{n_\rho}(t) \quad (\text{price/MA ratio}), \quad (20)$$

$$s_t^{(3)} := \nu_t := \log \frac{\hat{\sigma}_t^{\text{EWMA}}}{\hat{\sigma}_{n_{\text{LR}}, t}} \quad (\text{volatility regime}), \quad (21)$$

$$\underbrace{s_t^{(4a)} \text{ := RSI}_t}_{\text{RSI}} \quad \underbrace{s_t^{(4b)} \text{ := Hist}_t}_{\text{MACD}}, \quad (22)$$

$$s_t^{(5)} := v_{n_v}(t) \quad (\text{volume ratio}), \quad (23)$$

$$\underbrace{s_t^{(6a)} \text{ := \%b}_t}_{\text{BB position}} \quad \underbrace{s_t^{(6b)} \text{ := } a_t^{\text{rel}}}_{\text{ATR rel}}. \quad (24)$$

Here n_{LR} is a long-run window (e.g., days) for baseline volatility.

Angle encoding (min–max, train-split only). For any scalar channel z_t , define

$$\text{mm}(z_t; a, b) := \text{clip}\left(\frac{z_t - a}{b - a}, 0, 1\right), \quad a := \min_{\tau \in \mathcal{T}_{\text{train}}} z_\tau, \quad b := \max_{\tau \in \mathcal{T}_{\text{train}}} z_\tau, \quad (25)$$

$$\theta[z_t] := 2\pi \text{mm}(z_t; a, b). \quad (26)$$

The 6-qubit angle map uses one rotation per scalar channel, with two-axis encodings for composite channels:

$$\text{Initialize } |\psi_{\text{in}}\rangle = |0\rangle^{\otimes 6}. \quad (27)$$

$$\text{Qubit 1 (momentum)} : \quad R_y(\theta[s_t^{(1)}]), \quad (28)$$

$$\text{Qubit 2 (MA ratio)} : \quad R_y(\theta[s_t^{(2)}]), \quad (29)$$

$$\text{Qubit 3 (vol regime)} : \quad R_y(\theta[s_t^{(3)}]), \quad (30)$$

$$\text{Qubit 4 (RSI/MACD)} : \quad R_y(\theta[s_t^{(4a)}]) R_z(\theta[s_t^{(4b)}]), \quad (31)$$

$$\text{Qubit 5 (volume ratio)} : \quad R_y(\theta[s_t^{(5)}]), \quad (32)$$

$$\text{Qubit 6 (BB/ATR)} : \quad R_y(\theta[s_t^{(6a)}]) R_z(\theta[s_t^{(6b)}]). \quad (33)$$

This yields a feature-encoded state $|\psi_t\rangle := \text{U}_{\text{enc}}(t)|\psi_{\text{in}}\rangle$; a variational circuit $\text{U}_{\text{VQC}}(\phi)$ then acts on $|\psi_t\rangle$, and measured expectations $\langle Z_i \rangle$ feed the classical attention head as Q/K/V.

Models.

b) QASA mechanism: Given a token (or feature) vector $\mathbf{x}_t \in \mathbb{R}^d$, QASA uses three parameterized variational quantum circuits (VQCs) to produce query, key, and value:

$$Q_t = \text{VQC}_q(\mathbf{x}_t), \quad K_t = \text{VQC}_k(\mathbf{x}_t), \quad V_t = \text{VQC}_v(\mathbf{x}_t). \quad (34)$$

State preparation. For sequence inputs, we use amplitude encoding:

$$|\psi_t\rangle = \frac{1}{\|\mathbf{x}_t\|_2} \sum_{i=1}^d x_{t,i} |i\rangle. \quad (35)$$

For engineered features (hybrid variant), we may use angle encoding:

$$\theta_i = \frac{x_i - x_{\min}}{x_{\max} - x_{\min}} \cdot 2\pi, \quad (36)$$

and feed $\{\theta_i\}$ into the circuit as single-qubit parameterized rotations.

Variational circuit. On $n = \lceil \log_2 d \rceil$ qubits with L layers, a typical VQC block is

$$U(\theta) = \prod_{\ell=1}^L \left(\prod_{i=1}^n R_Y(\theta_{\ell,i}) \right) \left(\prod_{i=1}^{n-1} \text{CNOT}_{i,i+1} \right), \quad (37)$$

where $R_Y(\cdot)$ are parameterized rotations and CNOTs provide entanglement.

Measurement. Each VQC outputs an n -dimensional expectation vector by Pauli-Z measurements:

$$\text{VQC}(\mathbf{x}_t) = (\langle Z_1 \rangle, \dots, \langle Z_n \rangle), \quad \langle Z_i \rangle = \langle \psi_t | U^\dagger(\theta) Z_i U(\theta) | \psi_t \rangle. \quad (38)$$

Attention. Given the stacked matrices Q, K, V over a window (or mini-batch), QASA applies classical scaled dot-product attention:

$$\max_{\tau \in \mathcal{T}_{\text{train}}} z_\tau, \text{Attn}(Q, K, V) = \text{softmax}\left(\frac{QK^\top}{\sqrt{d_v}}\right) V, \quad (39)$$

with d_v the value dimension. The attention output is then fed to a shallow head for prediction.

QASA-Sequence: price windows \rightarrow VQC-generated Q/K/V \rightarrow attention \rightarrow classifier. ***QASA-Hybrid***: engineered features \rightarrow VQC Q/K/V \rightarrow attention. Baselines: RF, GB, Logistic Regression, Transformer, and pure quantum (VQE, QNN, QSVM).

QASA block. For token \mathbf{x}_t ,

$$\begin{aligned} Q_t &= \text{VQC}_q(\mathbf{x}_t), \quad K_t = \text{VQC}_k(\mathbf{x}_t), \\ V_t &= \text{VQC}_v(\mathbf{x}_t), \\ \text{Attn}(Q, K, V) &= \text{softmax}\left(\frac{QK^\top}{\sqrt{d}}\right)V. \end{aligned} \quad (40)$$

Expectation vectors are measured on n qubits after L layers of parameterized rotations and entanglers; attention outputs are decoded by a shallow head.

Metrics. Trading metrics: Total Return, Sharpe, Max Drawdown; classification metrics are recorded but omitted for space. Fees and cooldown are identical across models.

IV. EXPERIMENTAL SETUP

Task. Rebalancing as detection via the MA-anchored threshold in (1). We also consider alternative labels (concentrated-liquidity band and price-change thresholds) in ablations.

Data. Daily candles for BTCUSDC from 2024-01-01 to 2025-01-01 (about 252 trading days); 70/15/15 time-series split (train/val/test). Five-run repeats quantify uncertainty.

Features & quantum mapping. Engineered features include price/MA ratios, RSI/MACD, Bollinger/ATR, rolling/EWMA volatility, volume and microstructure proxies, lags, and interactions. Quantum inputs use angle encoding

$$\theta_i = \frac{x_i - x_{\min}}{x_{\max} - x_{\min}} \cdot 2\pi, \quad (41)$$

with a 6-qubit map covering momentum, MA ratios, volatility regime, RSI/MACD, volume ratios, and Bollinger/ATR position.

Models. *QASA-Sequence*: price windows \rightarrow VQC-generated Q/K/V \rightarrow attention \rightarrow classifier. *QASA-Hybrid*: engineered features \rightarrow VQC Q/K/V \rightarrow attention. Baselines: RF, GB, Logistic Regression, Transformer, and pure quantum (VQE, QNN, QSVM).

Metrics. Trading metrics: Total Return, Sharpe, Max Drawdown; classification metrics are recorded but omitted for space. Fees and cooldown are identical across models.

V. RESULTS

Classical ML in trading. Ensembles such as Random Forest (RF) and Gradient Boosting (GB) remain strong when coupled with rich features, achieving 9.8% average return and the highest *family-level* Sharpe (1.47) in our study.

Quantum ML. Pure quantum models (VQE classifier, QNN, QSVM) are attractive for nonlinear decision

TABLE I
MAIN BACKTESTING METRICS ON THE TEST SPLIT (JAN 2024–JAN 2025).

Model	Return	Sharpe	MaxDD
QASA Sequence	13.99%	1.76	-10.10%
Random Forest	13.16%	1.68	-8.21%
Gradient Boosting	12.31%	1.68	-8.10%
Transformer	11.73%	1.23	-8.21%
QASA Hybrid	11.91%	1.32	-1.70%

boundaries but under current constraints underperform on financial time series (4.4% avg. return; 0.83 Sharpe).

Attention & hybrids. Attention-based models (e.g., transformers) are competitive on sequences but may incur higher volatility; hybrid quantum–classical designs such as **QASA** integrate VQCs inside attention by producing quantum Q/K/V followed by classical softmax attention.

Family-level comparison. Hybrids average **11.2%** return and **Sharpe 1.42**, outperforming pure quantum (**4.4%; 0.83**) and close to classical (**9.8%; 1.47**). Transformer yields the highest average return (**12.3%**) with higher volatility.

Best single model. **QASA-Sequence** achieves **13.99%** return, **Sharpe 1.76**, **Calmar 6.51**, surpassing RF (13.16%, 1.68) and GB (12.31%, 1.68). **QASA-Hybrid** minimizes drawdown (**-1.70%**) while maintaining double-digit returns.

Uncertainty & efficiency. Over five runs, QASA-Sequence shows the highest mean with modest variance (return s.d. 2.04%); RF/GB are steadier. Complexity/efficiency analysis ranks ensembles most cost-effective; QASA-Hybrid provides a balanced mid-cost option; QASA-Sequence trades compute for peak Sharpe.

VI. CONCLUSION

Building on the *Quantum Adaptive Self-Attention (QASA)* block proposed in prior work [13] and related quantum self-attention designs [14], [26], we presented, to the best of our knowledge, the first application of QASA to DeFi by casting AMM rebalancing as a detection problem. In controlled 2024 backtests on three major cryptocurrency pairs with strict time-series splits and identical fee/cooldown settings, **QASA-Sequence** achieved the top risk-adjusted performance (Sharpe = 1.76) and the highest cumulative return (13.99%), while *QASA-Hybrid* variants offered a favorable balance among profitability, volatility, and drawdown relative to pure-quantum baselines. These findings indicate that *quantum-generated queries/values plugged into a classical attention head* is a practical and effective design for trading decision modules under noisy, regime-switching markets.

REFERENCES

- [1] H. Adams, N. Zinsmeister, M. Salem, R. Keefer, and D. Robinson, “Uniswap v3 core,” tech. rep., Uniswap, 2021. Technical whitepaper.

- [2] G. Angeris and T. Chitra, "Improved price oracles: Constant function market makers," in *Proceedings of the 2nd ACM Conference on Advances in Financial Technologies (AFT)*, 2020.
- [3] G. Angeris, A. Evans, and T. Chitra, "Replicating market makers," *Digital Finance*, vol. 5, no. 2, pp. 367–387, 2023.
- [4] J. Milionis, C. C. Moallemi, T. Roughgarden, and A. L. Zhang, "Quantifying loss in automated market makers," in *ACM CCS Workshop on Decentralized Finance and Security (DeFi'22)*, 2022.
- [5] L. Heimbach, E. Schertenleib, and R. Wattenhofer, "Risks and returns of uniswap v3 liquidity providers," in *Proceedings of the 4th ACM Conference on Advances in Financial Technologies (AFT)*, 2022.
- [6] M. Neuder, R. Rao, D. J. Moroz, and D. C. Parkes, "Strategic liquidity provision in uniswap v3," *arXiv preprint*, 2021.
- [7] J. D. Hamilton, "A new approach to the economic analysis of nonstationary time series and the business cycle," *Econometrica*, vol. 57, no. 2, pp. 357–384, 1989.
- [8] R. S. Tsay, *Analysis of Financial Time Series*, 3rd ed. Wiley, 2010.
- [9] A. Vaswani, N. Shazeer, N. Parmar, J. Uszkoreit, L. Jones, A. N. Gomez, L. Kaiser, and I. Polosukhin, "Attention is all you need," in *NeurIPS*, 2017.
- [10] Z. Zhang, S. Zohren, and S. Roberts, "Deeplob: Deep convolutional neural networks for limit order books," *IEEE Transactions on Signal Processing*, vol. 67, no. 11, pp. 3001–3012, 2019.
- [11] J. Wallbridge, "Translob: Transformer-based limit order book modeling," *arXiv preprint*, 2020.
- [12] B. Lim, S. Ö. Arik, N. Loeff, and T. Pfister, "Temporal fusion transformers for interpretable multi-horizon time series forecasting," *International Journal of Forecasting*, vol. 37, no. 4, pp. 1748–1764, 2021.
- [13] C.-S. Chen and E.-J. Kuo, "Quantum adaptive self-attention for quantum transformer models," *arXiv preprint arXiv:2504.05336*, 2025.
- [14] E. A. Cherrat, I. Kerenidis, N. Mathur, J. Landman, M. Strahm, and Y. Y. Li, "Quantum vision transformers," *Quantum*, vol. 8, p. 1265, 2024.
- [15] V. Havlíček, A. D. Córcoles, K. Temme, A. W. Harrow, A. Kandala, J. M. Chow, and J. M. Gambetta, "Supervised learning with quantum-enhanced feature spaces," *Nature*, vol. 567, pp. 209–212, 2019.
- [16] M. Schuld and N. Killoran, "Quantum machine learning in feature hilbert spaces," *Physical Review Letters*, vol. 122, no. 4, p. 040504, 2019.
- [17] M. Schuld, "Supervised quantum machine learning models are kernel methods," *PRX Quantum*, vol. 2, no. 3, p. 030301, 2021.
- [18] J. Preskill, "Quantum computing in the nisq era and beyond," *Quantum*, vol. 2, p. 79, 2018.
- [19] C.-S. Chen and A. H.-W. Tsai, "Benchmarking classical and quantum models for defi yield prediction on curve finance," *arXiv preprint arXiv:2508.02685*, 2025.
- [20] N. Stamatopoulos *et al.*, "Option pricing using quantum amplitude estimation," *Quantum*, vol. 4, p. 291, 2020.
- [21] H. Adams, N. Zinsmeister, and D. Robinson, "Uniswap v2 core," tech. rep., Uniswap, 2020. Technical whitepaper.
- [22] Z. Zhang, S. Zohren, and S. Roberts, "Deeplob: Deep convolutional neural networks for limit order books," *IEEE Transactions on Signal Processing*, vol. 67, no. 11, pp. 3001–3012, 2019.
- [23] J. Frank, "Forecasting realized volatility in turbulent times using temporal fusion transformers," tech. rep., FAU Discussion Papers in Economics, 2023.
- [24] C.-S. Chen and E.-J. Kuo, "Quantum-enhanced natural language generation: A multi-model framework with hybrid quantum-classical architectures," *arXiv preprint arXiv:2508.21332*, 2025.
- [25] G. Li, X. Zhao, and X. Wang, "Quantum self-attention neural networks for text classification," *arXiv preprint*, 2022.
- [26] G. Li, X. Zhao, and X. Wang, "Quantum self-attention neural networks for text classification," *Science China Information Sciences*, vol. 67, no. 4, p. 142501, 2024.